

Accurate Analysis of Light Scattering and Absorption by an Infinite Flat Grating of Thin Silver Nanostrips in Free Space Using the Method of Analytical Regularization

Tatiana L. Zinenko, *Member, IEEE*, Marian Marciniak, *Senior Member, IEEE*, and Alexander I. Nosich, *Fellow, IEEE*

Abstract—We study the plane wave scattering and absorption by a flat grating of thin silver nanostrips located in free space, in the visible-light range. The formulation involves generalized boundary conditions imposed on the strip median lines. We use an accurate numerical solution to this problem based on the dual-series equations and the method of analytical regularization. This guarantees fast convergence and controlled accuracy of computations. Reflectance, transmittance, and absorbance as a function of the wavelength and the grating parameters are analyzed. In addition to well-known surface-plasmon resonances, sharp resonances are revealed in the H-polarized scattering near but not equal to the Rayleigh wavelengths of nonzero diffraction orders; in the E-polarized scattering these resonances are not visible. Asymptotic formulas for the frequencies and natural fields of the grating resonances are presented.

Index Terms—Absorption, generalized boundary conditions (GBC), grating, resonances, scattering, silver nanostrip.

I. INTRODUCTION

GRATINGS in the form of flat periodic arrays of thin silver or gold strips (see Fig. 1) are used today across a wide range of optical and photonic applications. This is apparently conditioned by the relative simplicity of the manufacturing of metal strips by the existing etching and beam lithography techniques. Their applications frequently exploit the Hertz effect, i.e., high polarization selectivity [1], if the period is smaller than the wavelength. First discovered and widely used at microwaves, this effect is also present in the optical range, despite the larger losses and generally different behavior of the metal

Manuscript received July 31, 2012; revised October 25, 2012; accepted October 29, 2012. Date of publication November 15, 2012; date of current version April 25, 2013. This work was supported in part by the National Academy of Sciences of Ukraine via the State Target Program “Nanotechnologies and Nanomaterials” and in part by the European Science Foundation via the Research and Networking Programme “Plasmon-Nanobiosense.”

T. L. Zinenko is with the Department of Quasioptics, Institute of Radio Physics and Electronics, National Academy of Sciences of Ukraine, Kharkov 61085, Ukraine (e-mail: tzinenko@yahoo.com).

M. Marciniak is with the National Institute of Telecommunications, Warsaw 04-894, Poland, and also with the Kielce University of Technology, Kielce 25-314, Poland (e-mail: m.marciniak@itl.waw.pl).

A. I. Nosich is with the Laboratory of Micro and Nano Optics, Institute of Radio Physics and Electronics, National Academy of Sciences of Ukraine, Kharkov 61085, Ukraine (e-mail: anosich@yahoo.com).

Color versions of one or more of the figures in this paper are available online at <http://ieeexplore.ieee.org>.

Digital Object Identifier 10.1109/JSTQE.2012.2227685

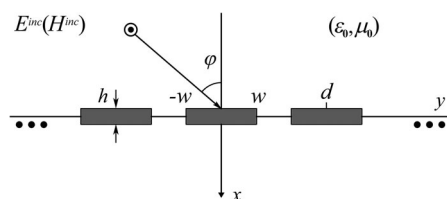


Fig. 1. Cross-sectional geometry of the silver strip grating scattering problem.

dielectric function. For instance, subwavelength gold strip gratings are used in the vertical-cavity semiconductor lasers for the polarization selection of modes.

Still many other optical applications of metal strips and their arrays relate to the localized surface-plasmon resonances (P-resonances for brevity) [2]. Its origin is explained by the fact that, for good metals in optical range, the leading contribution to the dielectric function comes from the collective oscillations of conduction electrons. As one can see, the P-resonance on thin strips ruins the Hertz effect for subwavelength-period strip grating. Since the 1990s, metal-strip gratings are widely used as substrates for biosensors and surface-enhanced Raman spectroscopy. More recently, they have appeared in advanced designs of nanoscale broadband composite absorbers for novel plasmonic solar cells.

Theoretical analysis of metal strip gratings was started by Lamb [3], who derived useful small-period approximations for the reflectance and transmittance of a perfectly electrically conducting (PEC) strip grating. An important step was done by Rayleigh [4], who introduced Floquet expansions that enable one to reduce the grating problem to a single period.

The early experiments with metal-strip gratings of larger periods had shown nontrivial behavior of reflectance and transmittance near to wavelength equal to period value [5]. In this case, the analysis can be performed only numerically. Among the techniques developed for building the numerical solutions to the scattering by the gratings of PEC, resistive and dielectric strips are the spectral Galerkin-moment method [6], the inverse Fourier transform (IFT) method [7], the singular integral equation (IE) method with projection to orthogonal polynomials [8], [9], and the method of the Riemann–Hilbert problem [10], [11]. The latter two techniques relate to the method of analytical regularization [12]. Their many advantages follow from the Fredholm second kind nature of the resultant matrix

equations. The main of them is the mathematically proven and fast convergence (possibility to reduce the error) if truncating the matrix and the right-hand part at progressively larger orders.

In simulations related to the optical applications, the analysis cannot benefit from the PEC approximation to the strip material. One of the early achievements was the mode-matching method in combination with surface-impedance description of the strips [13]. This is valid if the strip thickness considerably exceeds the skin-depth value, which is around 20 nm in the visible. Surface-impedance model was instrumental in the visualization of complicated resonant behavior of thick ($h > 50$ nm) metal-strip gratings in the H-polarization case [14], and simpler but still far from trivial behavior in the E-polarization case [15].

Another important numerical technique is the Fourier modal method, based on the series expansions of both the field and the dielectric function in the domain of grating. It was used in [16] and [17] to study optical resonances on the silver-strip gratings lying on thin dielectric substrates and on dielectric–air interface, respectively.

The goal of this paper is to apply the accurate meshless analytical–numerical approach, originally developed in [10] for the gratings made of resistive and conventional-dielectric strips, to the plane wave scattering by a flat grating of thin noble-metal nanostrands. Therefore, we avoid repeating all mathematical details of [10], and concentrate on the physics of resonance effects. In the visible range, one has to account accurately for the dispersion of the complex-valued bulk refractive index of silver $\nu(\lambda)$. We use the experimental data for its real and imaginary parts taken from [18], and apply Akima spline interpolation between the experimental values, to avoid inaccuracies brought by the Drude formulas.

The remainder of this paper is organized as follows. In Section II, we formulate the boundary value problem, reduce it to the dual-series equations, and perform their analytical regularization. Section III contains a numerical study of the scattering and absorption of the H and E-polarized plane waves. In Section IV, we obtain analytical formulas for the frequencies and natural fields of the grating resonances. Conclusions are formulated in Section V. Note that the time dependence is assumed as $e^{j\omega t}$ and omitted.

II. BASIC EQUATIONS

Consider the two-dimensional (2-D) scattering of a plane wave by a grating made of thin silver strips. The geometry of the problem is illustrated in Fig. 1. An infinite number of strips, parallel to the z -axis, are located in the plane $x = 0$ with period d . Each strip has the width $2w$. The propagation vector of the incident plane wave makes the angle φ with respect to the negative x -axis.

The field scattered by the grating should satisfy the Helmholtz equation and certain boundary conditions at the strip contours. Assuming that the nanostrand thickness is 10 or 20 nm, we can see that this is much smaller than the wavelength in the visible range (300 to 900 nm), so that $h \ll \lambda$. This justifies the use of the following set of “effective” or generalized boundary conditions (GBC) [19]–[24] involving only the limiting values of the field

components

$$\begin{aligned} & (1/2) \left[\vec{E}_T^+(0, y) + \vec{E}_T^-(0, y) \right] \\ & = Y^{(e)} \vec{x} \times \left[\vec{H}_T^+(0, y) - \vec{H}_T^-(0, y) \right] \\ & (1/2) \left[\vec{H}_T^+(0, y) + \vec{H}_T^-(0, y) \right] \\ & = -Y^{(m)} \vec{x} \times \left[\vec{E}_T^+(0, y) - \vec{E}_T^-(0, y) \right]. \end{aligned} \quad (1)$$

Here, the superscript \pm indicates the limiting value of the function at $x \rightarrow \pm 0$, the subscript T denotes vectors tangential to the strips, and \vec{x} is the unit vector normal to the strips. These GBC have been derived from the analysis of the plane-wave scattering by a thin infinite material layer in [19]–[24]. As the right-hand parts of (1) are identified as electric and magnetic currents, these conditions have the meaning of Ohm’s law for a thin material layer. They allow neglecting the fields inside the layer and characterizing its properties by means of coefficients $Y^{(e)}$ and $Y^{(m)}$, called electrical and magnetic resistivities, respectively. Following [23], we set

$$\begin{aligned} Y^{(e)} &= -(j\zeta_0/2\nu) \cot(\nu k_0 h/2) \\ Y^{(m)} &= -(j\nu/2\zeta_0) \cot(\nu k_0 h/2) \end{aligned} \quad (2)$$

where ζ_0 is the free-space impedance, h is the strip thickness, and $k_0 = 2\pi/\lambda$ is the free-space wavenumber. Here, the bulk refractive index of silver is linked to the relative dielectric function as $\varepsilon = \nu^2$. Generally, expressions (2) are valid for thin ($h \ll \lambda$) strips in the high-contrast case ($|\varepsilon| \gg 1$) that is true for a silver slab of 5- to 50-nm thickness in the visible range. For a thinner than 2-nm layer, the bulk values of silver refractive index should be corrected for the mean free path of electrons becoming comparable to the thickness—discussion about this was active in the early 2000’s [25]. Besides, it is useful to see that in the limit of $k_0 h \rightarrow \infty$ GBC (1), (2) “automatically” become the surface-impedance boundary conditions. In the visible range this happens with accuracy of 10^{-3} if $h \geq 100$ nm. Note that GBC have been successfully used in [26] and [27] in the analysis of scattering by thin stand-alone dielectric and metal strips. In [10], they were confronted with an algorithm based on the volume integral equation that did not assume the strips to be thin. Agreement was very good even in the resonances (see [10], Fig. 8).

For the uniqueness of solution of the scattering problem, we complete the formulation with the edge condition (local power finiteness) and the radiation condition at $x \rightarrow \pm\infty$ (outgoing and decaying behavior of diffraction orders).

Two alternative cases of the H-polarized (only H_z , E_x , and E_y are nonzero) and E-polarized wave scattering (only E_z , H_x , and H_y components are nonzero) can be considered similarly to each other. Denote the z -component of the corresponding field by $U(x, y)$ and introduce $\beta_0 = k_0 \sin \varphi$, $\alpha_0 = k_0 \cos \varphi$. Then, the incident wave is

$$U^{\text{inc}}(x, y) = \exp[-j(\alpha_0 x + \beta_0 y)]. \quad (3)$$

Due to periodicity of the boundary conditions, the z component of the scattered field is a quasi-periodic function of y and can be expanded in the Floquet series

$$U^{\text{scat}}(x, y) = \sum_{n=-\infty}^{\infty} \begin{cases} a_n^{H,E}, & x > 0 \\ b_n^{H,E}, & x < 0 \end{cases} \exp[-j(\alpha_n |x| + \beta_n y)] \quad (4)$$

where $\beta_n = \beta_0 + 2n\pi/d$, $\alpha_n = (\kappa_0^2 - \beta_n^2)^{1/2}$, and the radiation condition requires that either $\text{Re } \alpha_n > 0$ or $\text{Im } \alpha_n < 0$ for each n .

To determine the unknown Floquet-mode amplitudes of the scattered field in the transmission and reflection half-space, i.e., a_n and b_n , respectively, we use dual sets of conditions that hold on the complementary subintervals of the elementary period. They are GBC (1) on the metal-strip part M , and conditions of the field continuity $\vec{H}_T^+(0, y) = \vec{H}_T^-(0, y)$ and $\vec{E}_T^+(0, y) = \vec{E}_T^-(0, y)$ on the slot part S .

Substitution of the Floquet series (4) into dual conditions leads to two decoupled pairs of the dual-series equations (DSE). In the H-polarization case, they are

$$\begin{cases} \sum_{n=-\infty}^{\infty} (a_n - b_n) |n| e^{jn\psi} = 2r_0 \\ + \sum_{n=-\infty}^{\infty} (a_n - b_n) (r_n - 2j\kappa Y^{(e)}/\zeta_0) e^{jn\psi}, & |\psi| < \theta \\ \sum_{n=-\infty}^{\infty} (a_n - b_n) e^{jn\psi} = 0, & \theta < |\psi| \leq \pi \end{cases} \quad (5)$$

$$\begin{cases} \sum_{n=-\infty}^{\infty} (a_n + b_n) g_n e^{jn\psi} = -(Y^{(m)}\zeta_0)^{-1} \\ + (2Y^{(m)}\zeta_0)^{-1} \sum_{n=-\infty}^{\infty} (a_n + b_n) e^{jn\psi}, & |\psi| < \theta \\ \sum_{n=-\infty}^{\infty} (a_n + b_n) g_n e^{jn\psi} = 0, & \theta < |\psi| \leq \pi \end{cases} \quad (6)$$

where $g_n = [1 - (\sin \varphi + n/\kappa)^2]^{1/2}$, $\kappa = d/\lambda$, $r_n = |n| - jg_n\kappa$, $\psi = 2\pi y/d$, and $\theta = 2\pi w/d$. Similar equations for the E-polarization case can be found in [10].

Further, we perform analytical inversion of the *principal* parts of DSEs (5) and (6) in terms of the dependences on the summation index n using the RHP and IFT technique, respectively (see Appendix of [10]). This procedure leads to two decoupled infinite-matrix equations, together equivalent to the original boundary-value problem,

$$(I + A_{1,2}^H) X_{1,2} = B_{1,2}^H \quad (7)$$

$$I = \{\delta_{mn}\}_{m,n=-\infty}^{\infty}, \quad X_1 = \{d_n\}_{n=-\infty}^{\infty}, \quad X_2 = \{c_n\}_{n=-\infty}^{\infty}$$

$$A_{1,2}^H = \left\{ A_{1(2),mn}^H \right\}_{m,n=-\infty}^{\infty}$$

$$A_{1,mn}^H = (2j\kappa Y^{(e)}/\zeta_0 - r_n) S_{mn}^{(1)}(\theta)$$

$$A_{2,mn}^H = w_m (2Y^{(m)}\zeta_0 g_m w_n)^{-1} S_{mn}^{(2)}(\theta)$$

$$B_{1,2}^H = \left\{ B_{1(2),m}^H \right\}_{m=-\infty}^{\infty}, \quad B_{1,m}^H = 2r_0 S_{m0}^{(1)}(\theta)$$

$$B_{2,m}^H = w_m (Y^{(m)}\zeta_0 g_m)^{-1} S_{m0}^{(2)}(\theta).$$

Here, δ_{mn} stands for the Kronecker delta, and d_n and c_n are new coefficients depending on the unknown Floquet-mode amplitudes of the scattered field as $d_n = a_n - b_n$ and $c_n = (a_n + b_n)w_n$ where the weight $w_n = (|n| + 1)^{1/2}$ is introduced in order to balance the decay of matrix elements for $|n| \rightarrow \infty$ and $|m| \rightarrow \infty$. The expressions for $S_{mn}^{(1,2)}(\theta)$ involve only trigonometric functions (see also [29])

$$S_{mn}^{(1)}(\theta) = \frac{P_{m-1}(u)P_n(u) - P_m(u)P_{n-1}(u)}{2(m-n)}$$

$$S_{00}^{(1)}(\theta) = -\ln \frac{1+u}{2}$$

$$S_{mm}^{(1)}(\theta) = (2|m|)^{-1} \sum_{k=0}^{|m|} q_{|m|-k}(u) P_{|m|-k-1}(u), m \neq 0 \quad (8)$$

where $P_n(u)$ are the Legendre polynomials, $u = \cos \theta$, $q_0 = 1$, $q_1(u) = -u$, $q_{k>1}(u) = P_k(u) - 2uP_{k-1}(u) + P_{k-2}(u)$, and

$$S_{mn}^{(2)}(\theta) = -\frac{\sin \theta(m-n)}{\pi(m-n)}, m \neq n, \quad S_{mm}^{(2)}(\theta) = 1 - \frac{\theta}{\pi}. \quad (9)$$

As discussed in [10], the following inequalities hold true

$$\sum_{m,n=-\infty}^{\infty} \left| A_{(1,2),mn}^{E,H} \right|^2 < \infty, \quad \sum_{m=-\infty}^{\infty} \left| B_{(1,2),m}^{E,H} \right|^2 < \infty \quad (10)$$

Hence, each of (7) is a Fredholm second-kind matrix equation in the space of sequences l_2 , and therefore, the convergence is mathematically guaranteed when solving their finite-size counterparts. Note that all the elements of (7) are combinations of elementary functions, need no numerical integrations, and hence can be easily computed with machine precision. Then, the accuracy is controlled by the truncation number; we kept it at the level of 10^{-4} in the later presented numerical results that needed some 100 unknowns in each matrix equation.

To obtain similar solution for the E-wave case, $Y^{(m)}\zeta_0$ needs to be replaced with $Y^{(e)}/\zeta_0$, and vice versa in the DSE (5) and (6), and then in the matrix equations (7).

Reflectance and transmittance as fractions of power of the incident wave at a single period of grating are expressed as

$$R = g_0^{-1} \sum_{\text{Re } g_n > 0} g_n |b_n|^2, \quad T = g_0^{-1} \sum_{\text{Re } g_n > 0} g_n |a_n + \delta_{n0}|^2 \quad (11)$$

where summation is taken over the modes that carry power to infinity. These quantities and also the absorbance A are coupled by the optical theorem as $R + T + A = 1$.

III. NUMERICAL RESULTS

A. H-Polarization Scattering and Absorption

Fig. 2 demonstrates the reflectance, transmittance, and absorbance as a function of the wavelength for the scattering of

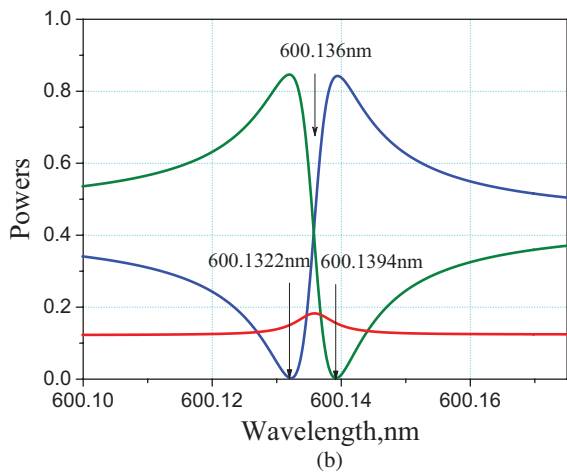
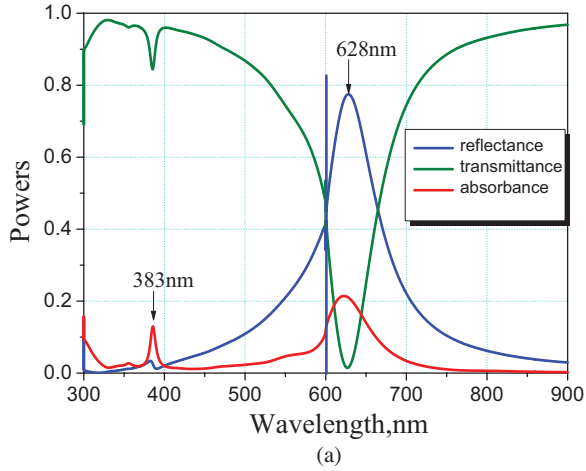


Fig. 2. Reflectance, transmittance, and absorbance as a function of the wavelength for the scattering of the H-wave from the grating of silver strips. $\varphi = 0^\circ$, $2w = 150$ nm, $d = 600$ nm, and $h = 10$ nm. Panel (b) is a zoom of (a).

the normally incident H-polarized (i.e., \vec{E} across the strips) plane wave, in the visible light range. One can see a number of resonances. They belong to two different types. The first one is broad P-resonances on silver strips (horizontal plasmon resonances of [17]). The grating of 150×10 -nm² strips demonstrates two P-resonances in the visible range: wide intensive peak at $\lambda^{P1} = 628$ nm and weaker peak at $\lambda^{P3} = 383$ nm. As shown in [28], they are associated with different Fabry–Perot orders of the same short-distance surface plasmon standing wave, bouncing between the strip edges. The near-field patterns in these resonances are shown in Figs. 3 and 4 and reveal the 1st and 3rd order resonances. Note that even-order P-resonances are not excited at the normal incidence.

The second type is G-resonances whose finesse is much higher. For the grating of period $p = 600$ nm at the normal incidence, only one of them appears in the visible range. It sits just above the wavelength of the ± 1 st Rayleigh’s anomaly (i.e., red shifted from it), at $\lambda^G = 600.136$ nm, on the green side of the broader P-resonance.

Zoom of the narrow vicinity of the G-resonance in Fig. 2(b) shows remarkable double-extremum Fano shape for R and T and small peak in A . The near-field pattern $|H_z|$ pattern in G-resonance

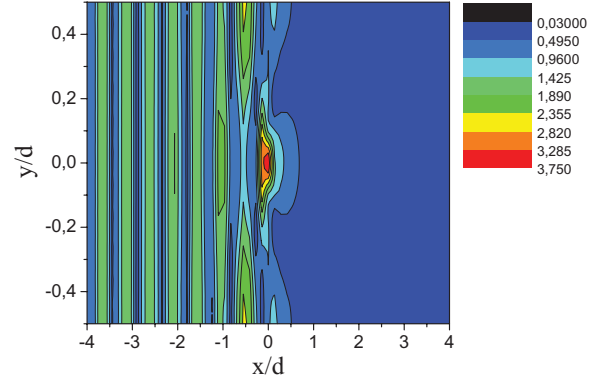


Fig. 3. Magnetic near-field pattern on elementary period for the scattering of the H-wave by the grating of silver strips in the plasmon resonance P_1 at $\lambda^{P1} = 628$ nm. Other parameters are the same as for Fig. 2.

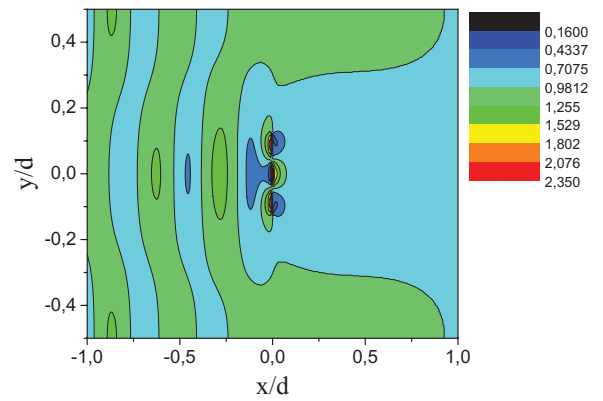


Fig. 4. Same as in Fig. 3 in the plasmon resonance P_3 at $\lambda^{P3} = 383$ nm.

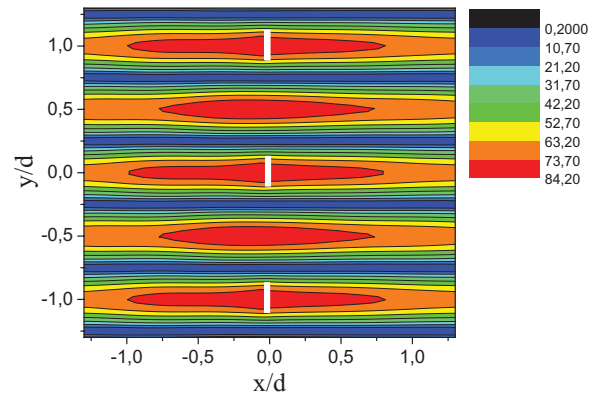


Fig. 5. Magnetic near-field pattern on three periods for the scattering of the H-wave from the grating of silver strips (marked by the white boxes) in the grating resonance at $\lambda^G = 600.136$ nm. Other parameters are as for Fig. 2.

is demonstrated in Fig. 5. It is drastically different from the plasmon resonances as it shows two extremely intensive maxima per period stretching very far (for some 45 periods) along the normal to the grating as can be seen in Fig. 6. This pattern will be explained in the next section.

As the G-resonance wavelength is conditioned by the grating period, one can “move” it to the first order P-resonance on the strip by adjusting the period to the plasmon-resonance wavelength [Fig. 7(a)]. Then, a zoom of the resonance range

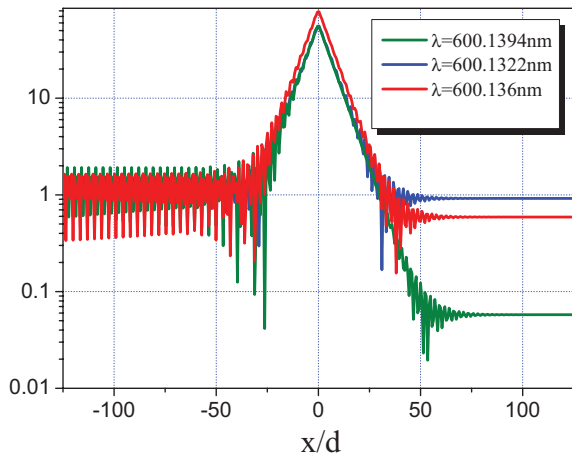


Fig. 6. Profile of the near-field magnitude along the line $y = 0$ for the scattering of the H-wave near the G-resonance at $\lambda^G = 600.136$ nm, $\lambda = 600.1322$ nm, and $\lambda = 600.1394$ nm. Other parameters are the same as for Fig. 2.

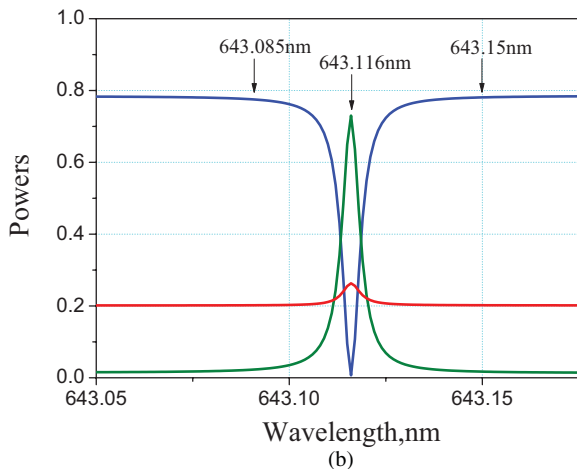
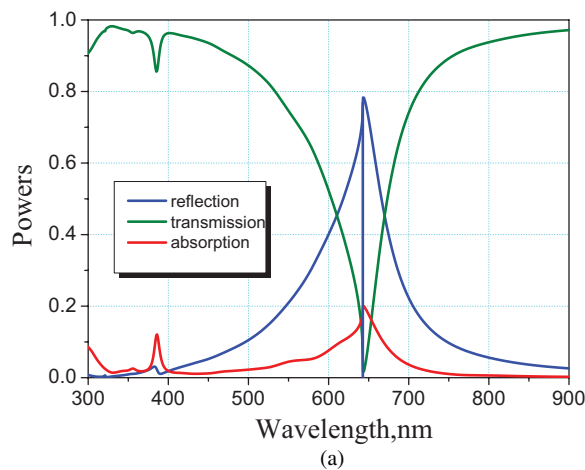


Fig. 7. Same as in Fig. 2 for $\varphi = 0^\circ$, $2w = 150$ nm, $d = 643$ nm, and $h = 10$ nm.

reveals the appearance of optically induced transparency: high-reflection band typical for the P-resonance is cut by a 1-pm narrow band of total transmission [see Fig. 7(b)].

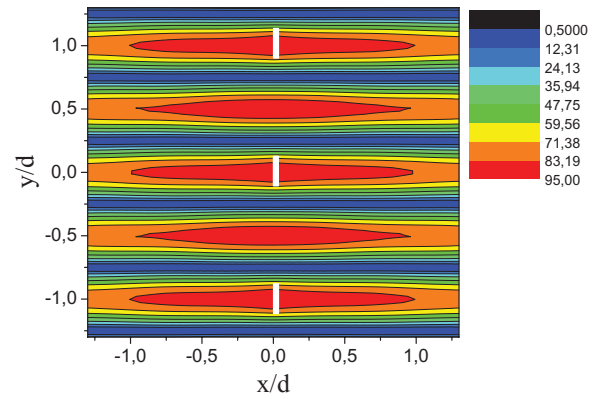


Fig. 8. Near-field pattern on three periods for the scattering of the H-wave from the grating of silver strips in the combined P-G resonance ($\lambda = 643.116$ nm). Other parameters are the same as for Fig. 7.

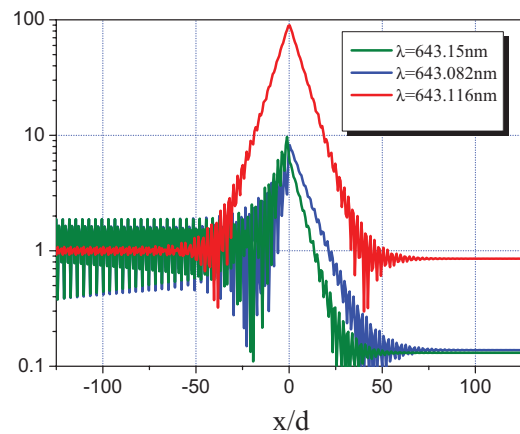


Fig. 9. Same as in Fig. 6 near to combined P-G resonance at $\lambda^P = 643.116$ nm, $\lambda = 643.082$ nm, and $\lambda = 643.15$ nm. Other parameters are the same as for Fig. 7.

Near-field pattern in this G-resonance shows familiar intensive standing wave along the y -axis (Fig. 8) with even larger peak values than in Fig. 5.

The field profiles cut along the x -axis (see Fig. 9) show that on the both sides of the narrow band of induced transparency the grating is well-reflective: far in the backward half-space ($x < -50d$) a standing wave is visible with field peak values around 2 while far in the forward half-space ($x > +50d$) there is a deep shadow. The most dramatic near-field enhancement is observed exactly at the wavelength of G-resonance, i.e., when the grating is totally transparent.

In the case of inclined incidence of the H-polarized plane wave, the scattering and absorption by the silver-strip grating becomes more complicated. This is because, unlike the normal incidence, the scattered field obtains the part that is antisymmetric across the x -axis (i.e., the line $y = 0$). The consequences are twofold: first, the even-order P-resonances can now be excited on the strips. Second, the Rayleigh wavelengths become different for the positive and negative diffractive orders (Floquet harmonics) and each of them is now accompanied, on the red side, by a sharp G-resonance [see Fig. 10(a)], where the resonances are identified as GH_{-2} , P_2 , GH_{-1} , P_1 , and GH_{+1}

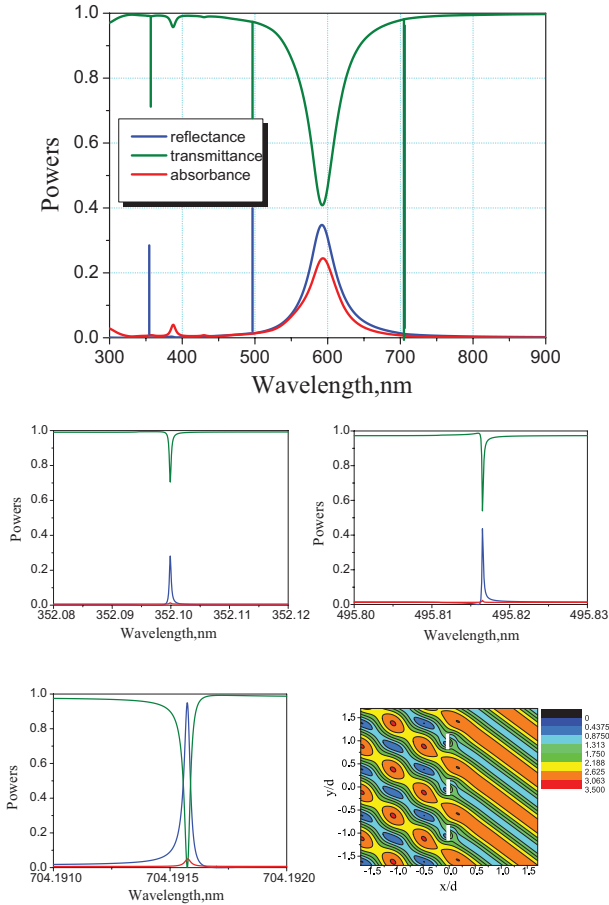


Fig. 10. Reflectance, transmittance, and absorbance as a function of the wavelength for the scattering of the H-wave from the grating of silver strips. $\varphi = 10^\circ$, $2w = 150$ nm, $d = 600$ nm, and $h = 5$ nm. (a) Full range; (b), (c), and (d) zooms of the G-resonances; and (e) H-field pattern in the GH_{+1} resonance.

At the inclined incidence, in-resonance near field [see Fig. 10(e)] shows a correspondingly inclined bright spot pattern.

B. E-Polarization Scattering and Absorption

The scattering of the E-polarized (i.e., \vec{E} along the strips) visible light by a flat grating of thin silver strips has attracted much smaller attention of researchers, apparently because of the absence of P-resonances. Still [15] dealt only with thick strips placed on a thin dielectric slab, and [16] with thin strips on a thick slab. The latter study had revealed sharp resonances near to the Rayleigh wavelengths of the slab medium. They were attributed to the “substrate modes” because they were not observed if the slab was thinner than certain value. As we study the free-standing grating (no substrate), we can clarify the role of supporting dielectric slab.

Fig. 11 demonstrates the plots of transmittance, reflectance, and absorbance versus the wavelength for the scattering of the normally incident E-polarized plane wave by three gratings of thin silver strips of different thickness. Neither P-resonances nor G-resonances are seen; however, the curves have sharp maxima (minima) exactly at the wavelength of Rayleigh anomaly, i.e., at 600 nm.

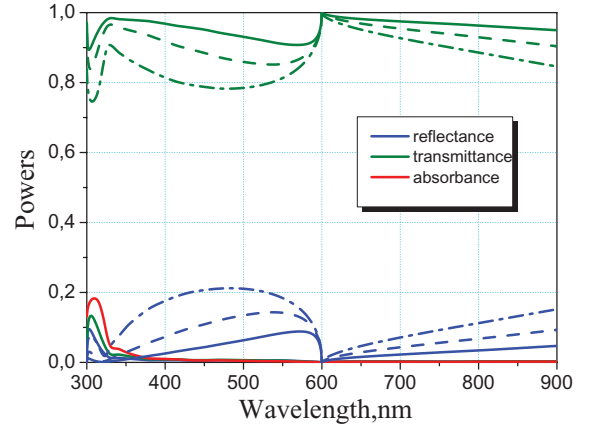


Fig. 11. Reflectance, transmittance, and absorbance as a function of the wavelength for the scattering of the E-wave from the grating of silver strips. $\varphi = 0^\circ$, $d = 600$ nm, $h = 10$ nm (solid lines), 20 nm (dashed lines), and 50 nm (dash-dotted lines).

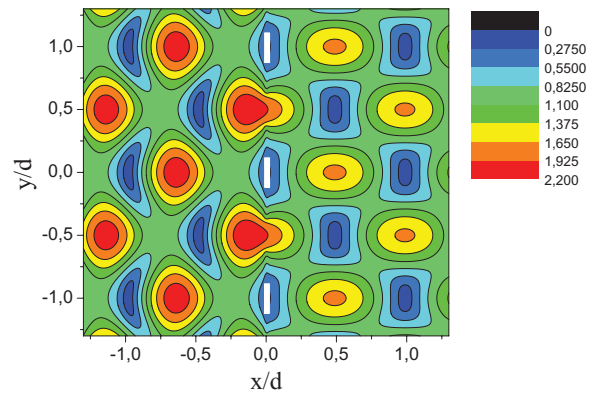


Fig. 12. Electric near-field pattern on three periods for the scattering of the e-wave from the grating of silver strips at $\lambda = 600.01$ nm. $\varphi = 0^\circ$, $2w = 150$ nm, $d = 600$ nm, and $h = 10$ nm.

The absence of resonances means that there is no near-field enhancement that is certified by the pattern presented in Fig. 12. The electric field is close to zero near to the silver strips and has maximum value of only 2.2 between them.

IV. GRATING MODES

Any grating is a periodic open resonator whose complex-valued natural frequencies $\kappa = d/\lambda$ form a discrete set coinciding with the roots of full-wave determinantal equations, $\text{Det}[I + A_{1,2}^{H,E}(\kappa)] = 0$. The Fredholm nature of (7), together with Gerschgorin theorem, ensures that these eigenvalues lie in finite circles centred at the zeros of the diagonal elements, i.e., roots of $1 + A_{(1,2)mm}^{H,E}(\kappa) = 0$. This property leads to the following equations:

$$1 + (2Y^{(e,m)}g_m)^{-1}S_{mm}^{(1,2)}(\theta) = 0, \quad m = \pm 1, \pm 2, \dots \quad (12)$$

Assuming that $\tilde{h} = h/d \rightarrow 0$, in the H-polarization case we have

$$[(m - \kappa \sin \varphi)^2 - \kappa^2]^{1/2} \approx \theta \tilde{h} \kappa^2. \quad (13)$$

For arbitrary m and φ , (13) has two roots. At the normal incidence ($\varphi = 0$) they merge together and correspond to double

degenerate natural frequencies of the $GH_{\pm m}$ resonances

$$\kappa_m^{GH} = m - m^3(\theta\tilde{h})^2 + O(|\varepsilon|m^4\tilde{h}^4). \quad (14)$$

In the case of E-polarization, similar treatment yields

$$\kappa_m^{GE} = m - m^3(|\varepsilon|\tilde{h})^2 + O(|\varepsilon|^3m^4\tilde{h}^4). \quad (15)$$

It should be stressed that, according to (14) and (15), G-modes as specific poles of the field as a function of wavelength are present on the gratings of both conventional dielectric strips and noble-metal strips, and in the both of two alternative polarizations (see [10] and [11]). This is drastically different from the P-resonances, which exist only on noble-metal wires or strips and only in the case of H-polarization. Therefore it is misleading to call them “nonradiative plasmons,” “collective plasmons,” etc. (see [30] for discussion). They should be also distinguished from the Rayleigh anomalies ($\kappa = m$, at the normal incidence), which correspond to the field branch points in κ .

Equation (14) correctly predicts the locations of the G-resonances seen in Figs. 2, 7 and 10. The estimation of the natural-mode quality-factors, $Q_m = |\operatorname{Re} \kappa_m / 2\operatorname{Im} \kappa_m|$, needs derivation of the next terms in (14) and (15). However, even from the comparison of the values of neglected terms one can see that for the silver strips in the H-polarization case $Q_m^{GH} \sim O(|\varepsilon|^{-1}m^{-4}\tilde{h}^{-4})$ that is $|\varepsilon|^2$ times larger than in the E-case. The most interesting feature of G-modes is that if the strips get thinner, $\tilde{h} \rightarrow 0$, then the complex natural frequencies tend to Rayleigh frequencies, which are real valued both for lossless and lossy strip materials. As a consequence the associated Q-factors grow as $O(\tilde{h}^{-4})$ although the large value of silver $|\varepsilon|$ hinders this growth in the E-polarization case. This is the reason that G-resonances are not observed on the plots in Fig. 11.

If the incident wave length approaches the real part of the m th G-mode frequency, then the m th Floquet-harmonic amplitude takes a large value. However it still remains a slow wave, exponentially decaying in the normal direction as $\operatorname{Re} \kappa_m < m$. In this case, under the normal incidence, the grating vicinity is dominated by intensive standing wave built of two identical Floquet harmonics with numbers $+m$ and $-m$. For the plots in Figs. 5, 6, 8, and 9, $m = 1$ and hence

$$U^{sc} \approx 2a_1 e^{ik\alpha_1|x|} \cos(k\beta_1 y) \approx Q_1^{GH} \exp\left(-\frac{|x/d|}{Q_1^{GH}}\right) \cos \frac{2\pi y}{d}. \quad (16)$$

Note that the amplitudes $a_{\pm 1} \approx b_{\pm 1}$ of the ± 1 st Floquet harmonics are proportional to the G-mode Q-factor and not restricted by the optical theorem. This explains the near-field behavior observed in the mentioned figures.

It should be noted that recently very sharp G-resonances were reported in the analysis of the electromagnetic wave scattering by thick gratings ($h \geq 500$ nm) made of imperfect-metal bars of rectangular cross section [31]–[33] (nearly overlooked in the earlier study of [13]). Identified as Fabry–Perot resonances, they are in fact the same as “vertical plasmons” of [17]. Note that in [32], it has been explicitly emphasized that their nature is linked to the periodicity; however, they should not be mixed up with Rayleigh anomalies. Our accurate study demonstrates

that these resonances 1) exist even if the strip thickness tends to zero and hence cannot be associated with “vertical Fabry–Perot” effect and 2) correspond to the specific complex-valued poles of the field as a function of the wavelength. According to [31], [32] they can be explained using simple circuit-theory description that reveals their similarity to the G-resonances on the grating of PEC strips backed with a thin dielectric substrate [34].

V. CONCLUSION

We have presented mathematically grounded and numerically accurate results for the scattering and absorption of the H- and E-polarized plane waves by a sparse infinite flat grating of thin silver nanostrips suspended in air. This was achieved by using a meshless combination of the GBC on the strips, dual-series equations, and the method of analytical regularization. Using this accurate computational instrument, we have studied two types of resonance reflection and transmission in the H-polarization case: plasmon-type and grating-type, and enhanced transmission at the Rayleigh wavelengths in the E-polarization case. We have focused our computations on the sparse gratings, in which the strip width is noticeably smaller than the period.

P-resonances appear as broad peaks in the reflectance and correspond to the Fabry–Perot bouncing of the short-range surface plasmon wave between the strip edges. They have low Q-factors determined by the losses in silver. G-resonances are caused by the periodicity and hence very different: they have almost no dispersion as $\lambda_m^G = d/m + O(mh^2)$, and their Q-factors tend to infinity if the strip thickness gets smaller. If well separated from a P-resonance, the G-resonance displays Fano shapes (intensive reflection followed by zero reflection, or vice versa). If two resonances are brought together, then G-resonance leads to narrow-band induced transparency on top of a broader high reflectance band associated with P-resonance.

P-resonances have bright spots along the strips. In the case of G-resonance, the near field is drastically different. It is dominated by a wave standing along the grating as $\cos(2\pi my/d)$, with bright spots at the strips and between them that have amplitudes proportional to Q-factor. Thus, the champion values of the near-field enhancement for a silver-strip grating are reached not in the classical P-resonances, but in the G-resonances that have completely different nature. It is the latter resonances that should be considered as primary candidates for applications in biosensors, lasers, and photovoltaic devices.

REFERENCES

- [1] H. Hertz, “Ueber strahlen elektrischer kraft,” *Ann. Phys. Chem. Leipzig*, vol. 36, pp. 769–783, 1889.
- [2] G. Schider, J. R. Krenn, W. Gotschy, B. Lambrecht, H. Ditlbacher, A. Leitner, and R. F. Aussenegg, “Optical properties of Ag and Au nanowire gratings,” *J. Appl. Phys.*, vol. 90, no. 8, pp. 3825–3830, 2001.
- [3] H. Lamb, “On the reflection and transmission of electric waves by a metallic grating,” *Proc. Lond. Math. Soc.*, vol. 29, pp. 523–544, 1898.
- [4] L. Rayleigh, “On the dynamical theory of gratings,” in *Proc. R. Soc. Lond.*, 1907, vol. A-79, pp. 399–416.
- [5] W. K. Pursley, “The transmission of electromagnetic radiation through wire gratings,” Eng. Res. Inst., Univ. Michigan, Ann Arbor, Tech. Report Project 2351, 1956.

- [6] R.C. Hall and R. Mittra, "Scattering from a periodic array of resistive strips," *IEEE Trans. Antenna Propag.*, vol. 33, no. 9, pp. 1009–1011, Sep. 1985.
- [7] R. Petit and G. Tayeb, "Theoretical and numerical study of gratings consisting of periodic arrays of thin and lossy strips," *J. Opt. Soc. Amer. A, Opt. Image Sci.*, vol. 7, no. 9, pp. 1686–1692, 1990.
- [8] A. Matsushima, T. L. Zinenko, H. Minami, and Y. Okuno, "Integral equation analysis of plane wave scattering from multilayered resistive strip gratings," *J. Electromagn. Waves Appl.*, vol. 12, pp. 1449–1469, 1998.
- [9] T. L. Zinenko, A. Matsushima, and Y. Okuno, "Scattering and absorption of electromagnetic plane waves by a multilayered resistive strip grating embedded in a dielectric slab," *Trans. Inst. Electron. Inf. Commun. Eng.*, vol. E82-C, no. 12, pp. 2255–2264, 1999.
- [10] T. L. Zinenko, A. I. Nosich, and Y. Okuno, "Plane wave scattering and absorption by resistive-strip and dielectric-strip periodic gratings," *IEEE Trans. Antenn. Propag.*, vol. 46, no. 10, pp. 1498–1505, Oct. 1998.
- [11] T. L. Zinenko and A. I. Nosich, "Plane wave scattering and absorption by flat gratings of impedance strips," *IEEE Trans. Antennas Propag.*, vol. 54, no. 7, pp. 2088–2095, Jul. 2006.
- [12] A. I. Nosich, "Method of analytical regularization in the wave-scattering and eigenvalue problems: Foundations and review of solutions," *IEEE Antennas Propag. Mag.*, vol. 42, no. 3, pp. 25–49, Jun. 1999.
- [13] H. Lochbihler and R. Depine, "Highly conducting wire gratings in the resonance region," *Opt. Commun.*, vol. 32, no. 19, pp. 3459–3465, 1993.
- [14] J. M. Steele, C. E. Moran, A. Lee, C. M. Aguirre, and N. J. Halas, "Metal-dielectric gratings with subwavelength slots: Optical properties," *Phys. Rev. B*, vol. 68, no. 20, pp. 205103-1–205103-7, 2003.
- [15] H. Lochbihler, "Enhanced transmission of TE polarized light through wire gratings," *Phys. Rev. B*, vol. 79, no. 24, pp. 245427–245435, 2009.
- [16] A. Christ, T. Zentgraf, J. Kuhl, S. G. Tikhodeev, N. A. Gippius, and H. Giessen, "Optical properties of planar metallic photonic crystal structures: Experiment and theory," *Phys. Rev. B*, vol. 70, no. 12, pp. 125113-1–125113-15, 2004.
- [17] M. R. Gadsdon, I. R. Hooper, and J. R. Sambles, "Optical resonances on sub-wavelength lamellar gratings," *Opt. Exp.*, vol. 16, no. 26, pp. 22003–22028, 2008.
- [18] P. B. Johnson and R. W. Christy, "Optical constants of the noble metals," *Phys. Rev. B*, vol. 6, pp. 4370–4378, 1972.
- [19] K. M. Mitzner, "Effective boundary conditions for reflection and transmission by an absorbing shell of arbitrary shape," *IEEE Trans. Antennas Propag.*, vol. 16, pp. 706–712, 1968.
- [20] R. F. Harrington and J. R. Mautz, "An impedance sheet approximation for thin dielectric shells," *IEEE Trans. Antenn. Propag.*, vol. 36, pp. 531–534, 1975 (in fact, this paper deals with the resistive-sheet approximation).
- [21] G. A. Grinberg, "Boundary conditions for the electromagnetic field in the presence of thin metallic shells," *Radio Eng. Electron.*, vol. 26, no. 12, pp. 2493–2499, 1981.
- [22] G. Bouchitté, "Analyse limite de la diffraction d'ondes électromagnétiques par une structure mince," *C.R. Acad. Sci Paris, Ser II*, vol. 311, pp. 51–56, 1990.
- [23] E. Bleszynski, M. Bleszynski, and T. Jaroszewicz, "Surface-integral equations for electromagnetic scattering from impenetrable and penetrable sheets," *IEEE Antenn. Propag. Mag.*, vol. 35, no. 6, pp. 14–25, Dec. 1993.
- [24] A. Karlsson, "Approximate boundary conditions for thin structures," *IEEE Trans. Antenn. Propag.*, vol. 57, no. 1, pp. 144–148, Jan. 2009.
- [25] J. P. Kottmann and O. J. F. Martin, "Plasmon resonances of silver nanowires with a non-regular cross section," *Phys. Rev. B*, vol. 64, no. 23, pp. 5402–5412, 2001.
- [26] O. V. Shapoval, R. Sauleau, and A. I. Nosich, "Scattering and absorption of waves by flat material strips analyzed using generalized boundary conditions and Nystrom-type algorithm," *IEEE Trans. Antenn. Propag.*, vol. 59, no. 9, pp. 3339–3346, Sep. 2011.
- [27] O. V. Shapoval, R. Sauleau, and A. I. Nosich, "Modeling of plasmon resonances of multiple flat noble-metal nanostrips with a median-line integral equation technique," *IEEE Trans. Nanotechnol.*, vol. 12, 2013, to be published.
- [28] G. D. Valle, T. Søndergaard, and S. I. Bozhevolnyi, "Plasmon-polariton nano-strip resonators: From visible to infra-red," *Opt. Exp.*, vol. 16, no. 10, pp. 6867–6876, 2008.
- [29] A. I. Nosich, "Green's function-dual series approach in wave scattering from combined resonant scatterers," in *Analytical and Numerical Methods in Electromagnetic Wave Theory*, M. Hashimoto, M. Idemen, and O. A. Tretyakov, Eds. Tokyo, Japan: Science House, 1993, ch. 9, pp. 419–469.
- [30] D. M. Natarov, V. O. Byelobrov, R. Sauleau, T. M. Benson, and A. I. Nosich, "Periodicity-induced effects in the scattering and absorption of light by infinite and finite gratings of circular silver nanowires," *Opt. Express*, vol. 19, no. 22, pp. 22176–22190, 2011.
- [31] F. Medina, F. Mesa, and D. C. Skigin, "Extraordinary transmission through arrays of slits: A circuit theory model," *IEEE Trans. Microw. Theory Tech.*, vol. 58, no. 1, pp. 105–115, Jan. 2010.
- [32] V. Delgado and R. Marques, "Surface impedance model for extraordinary transmission in 1D metallic and dielectric screens," *Opt. Exp.*, vol. 19, no. 25, pp. 25290–25297, 2011.
- [33] H. Lochbihler and R. A. Depine, "Properties of TM resonances on metallic slit gratings," *Appl. Opt.*, vol. 51, no. 11, pp. 1729–1741, 2012.
- [34] R. Rodríguez-Berral, F. Medina, F. Mesa, and M. García-Vigueras, "Quasi-analytical modeling of transmission/reflection in strip/slit gratings loaded with dielectric slabs," *IEEE Trans. Microw. Theory Tech.*, vol. 60, no. 3, p. 405–418, Mar. 2012.



Tatiana L. Zinenko (M'00) was born in Alchevsk, Ukraine. She received the M.S. degree in radio physics from the Kharkiv National University, Kharkiv, Ukraine, the D.Eng. degree in system science from the Kumamoto University, Kumamoto, Japan, in 2000, and the Ph.D. degree in radio physics from the Institute of Radio Physics and Electronics, the National Academy of Sciences of Ukraine (IRE NASU), Kharkov, Ukraine, in 2004.

She joined the IRE NASU, where she is currently a Research Scientist. From 1996 to 2000, she was with the Department of Computer and Electrical Engineering, Kumamoto University, Kumamoto, Japan, as a Research Student. In 1999, she was a recipient of the SUMMA Graduate Student Fellowship in advanced electromagnetics. Her research interests include integral equation methods and electromagnetic wave scattering from imperfect scatterers and periodic gratings.

Marian Marciniak (M'94–SM'02) was born in Czarkowka Mala, Poland, in 1949. He received the M.S. degree in physics from the M. Curie-Skłodowska University, Lublin, Poland, in 1977, the Ph.D. degree in optoelectronics from the Military University of Technology, Warsaw, Poland, in 1989, and the D.Sc. degree in optics from the Warsaw University of Technology, Warsaw, Poland, in 1997.

From 1978 to 1997, he was with the Military Academy of Telecommunications, Zegrze, Poland. In 1996, he joined the National Institute of Telecommunications, Warsaw, where he is currently a Professor. Since 2008, he has been a Professor at Kielce University of Technology, Kielce, Poland. His research interests include photonics, subwavelength optics, optical waveguide theory and numerical modeling, beam-propagation methods, and nonlinear optical phenomena.

Dr. Marciniak was the originator of accession of Poland to European Research Programs in the photonics domain and served as Chairman of COST Action: "Towards functional sub-wavelength photonic structures." He is the originator and organizer of the international conference series on Transparent Optical Networks (ICTON) in Poland and EU starting from 1999. In 2001, he organized the IEEE Photonics Society Poland Chapter.



Alexander I. Nosich (M'94–SM'95–F'04) was born in Kharkiv, Ukraine, in 1953. He received the M.S., Ph.D., and D.Sc. degrees in radio physics from the Kharkiv National University, Kharkiv, in 1975, 1979, and 1990, respectively.

Since 1979, he has been with the Institute of Radio Physics and Electronics, National Academy of Science of Ukraine, Kharkov, Ukraine, where he is currently a Professor and Principal Scientist. Since 2010, he has been the Head of the Laboratory of Micro and Nano Optics initiated by him at this institute. Since 1992, he has been a Guest Fellow and Professors in the EU, Japan, Singapore, and Turkey. His research interests include the method of analytical regularization, propagation and scattering of waves, simulation of lasers, open waveguides, and antennas, and the history of microwaves.

Dr. Nosich was one of the initiators and Technical Committee Chairman of the international conference series on mathematical methods in electromagnetic theory (MMET) held in Ukraine in 1990–2012. In 1995, he organized the IEEE East Ukraine Joint Chapter, one of the first in the former U.S.S.R. From 2001 to 2003, he represented Ukraine in the European Microwave Association. Since 2008, he has been representing Ukraine in the European Association on Antennas and Propagation.